Biochemical and Biophysical Research Communications 454 (2014) 7–11

Contents lists available at ScienceDirect

Biochemical and Biophysical Research Communications

journal homepage: www.elsevier.com/locate/ybbrc

Comparison of the biological effects of ^{18}F at different intracellular levels

Genro Kashino [a,*], Kazutaka Hayashi [a], Kazumasa Douhara [a], Shinko Kobashigawa [b], Hiromu Mori [b]

[a] Advanced Molecular Imaging Center, Faculty of Medicine, Oita University, 1-1 Idaigaoka, Hasama-machi, Yufu City, Oita 879-5593, Japan
[b] Department of Radiology, Faculty of Medicine, Oita University, 1-1 Idaigaoka, Hasama-machi, Yufu City, Oita 879-5593, Japan

ARTICLE INFO

Article history:
Received 26 September 2014
Available online 6 October 2014

Keywords:
FDG-PET
DNA DSB
Radiobiology
Positron

ABSTRACT

We herein examined the biological effects of cells treated with ^{18}F labeled drugs for positron emission tomography (PET). The relationship between the intracellular distribution of ^{18}F and levels of damaged DNA has yet to be clarified in detail. We used culture cells (Chinese Hamster Ovary cells) treated with two types of ^{18}F labeled drugs, fluorodeoxyglucose (FDG) and fluorine ion (HF). FDG efficiently accumulated in cells, whereas HF did not. To examine the induction of DNA double strand breaks (DSB), we measured the number of foci for 53BP1 that formed at the site of DNA DSB. The results revealed that although radioactivity levels were the same, the induction of 53BP1 foci was stronger in cells treated with ^{18}F-FDG than in those treated with ^{18}F-HF. The clonogenic survival of cells was significantly lower with ^{18}F-FDG than with ^{18}F-HF. We concluded that the efficient accumulation of ^{18}F in cells led to stronger biological effects due to more severe cellular lethality via the induction of DNA DSB.

1. Introduction

Fluorine 18 (^{18}F) is a positron emitted radioisotope that is used for diagnoses with positron emission tomography (PET) [1–5]. Fluorodeoxyglucose (FDG), which is labeled with ^{18}F, is widely used in PET [5]. Not only FDG, but also other PET drugs labeled with ^{18}F are useful for estimating metabolic functions such as tumorigenesis [6,7], receptor occupancy [8–12], and the accumulation of beta amyloid [13–15]. Absorbed dose levels by positron and γ-rays in organs from the positron emission of ^{18}F must be considered in order to determine the risks associated with using ^{18}F in combination with PET drugs in terms of radiation exposure in the human body [16,17]. The half-life time of ^{18}F (= 110 min) and the pharmaceutical compartment model for each characteristic of a PET drug in each organ are the main factors that are used to estimate exposure levels in organs [18]. However, the main target of radiation from ^{18}F is thought to be the nucleus (DNA); therefore, it is important to estimate exposure levels in DNA using individual cell models. A clearer understanding of the intracellular distribution of ^{18}F is also needed because the induction of DNA damage, which is the main target of biological effects, is dependent on the number of radiation tracks emitted from ^{18}F. However, the relationship between the intracellular distribution of and level of DNA damage induced by ^{18}F remains unknown.

The extent of DNA double strand breaks (DSB), which is a useful indicator of irradiation levels, can be detected by the focus formation of phosphorylated H2AX (γ-H2AX) using an immunofluorescent assay [19–21]. The focus formation of γ-H2AX with other proteins has been attributed to the assembly of factors such as phosphorylated ATM (Ataxia telangiectasia mutated), MDC1 (Mediator of DNA damage checkpoint protein 1), and 53BP1 (Tumor suppressor p53-binding protein 1) [22,23]. These proteins are known to be mobilized by chromatin remodeling following DNA DSB [20,24]. Therefore, the formation of these foci is used as markers to estimate DNA DSB.

^{18}F-Fluorodeoxyglucose (FDG) is an analog of glucose. In culture cell lines such as the Chinese hamster ovary (CHO) cell line, cells exponentially grow in the culture dish; therefore, FDG and glucose are effectively incorporated into these cells. The phosphorylation of FDG by hexokinase then occurs in the glycolysis pathway. However, the phosphorylated form of FDG does not proceed in glycolysis, which leads to its accumulation in cells. On the other hand, the ion form of ^{18}F is composed of ^{18}O–H_2O from a nuclear reaction with a proton from a cyclotron accelerator. This ion form of ^{18}F is thought to be accessible to the inside of cells, but cannot accumulate there. Therefore, two different cellular distribution types exist for ^{18}F from FDG and fluorine ions.

We herein determined the induction of DNA DSB by two PET drugs carrying ^{18}F at individual cell levels, and found that the lethal effects induced by FDG were higher than those by fluoric ions in spite of the same levels of radioactivity. These results suggest that

* Corresponding author. Fax: +81 97 586 6314.
E-mail address: kashino@oita-u.ac.jp (G. Kashino).

http://dx.doi.org/10.1016/j.bbrc.2014.09.136
0006-291X/

the intracellular distribution of ^{18}F should be considered in order to estimate exposure at the cellular level.

2. Material and methods

2.1. Cell culture

Wild type CHO cells and the Ku80-deficient X-ray sensitive CHO cell line, xrs5, were kindly supplied by Dr. Tom K. Hei (Columbia University). Cells were cultured in MEM alpha medium (Invitrogen Ltd) supplemented with 10% FBS (HyClone Laboratories). Cells were maintained at 37 °C in a humidified atmosphere with 5% CO_2.

2.2. PET drugs

Fluorine 18 (^{18}F) was produced by a nuclear reaction between ^{18}O (p, n) and ^{18}F using a cyclotron system (Cypris HM-20s, Sumitomo Heavy Industries, Ltd., Tokyo, Japan). The fluorine 18 ion in H_2O (^{18}F-HF solution) was directly obtained from the cyclotron and diluted to approximately 400 MBq/ml. The ^{18}F-FDG solution was synthesized and purified using an automatic radiochemical synthesizer (F-300, Sumitomo Heavy Industries, Ltd.), and the radioactivity of ^{18}F was diluted by water to approximately 400 MBq/ml. Radioactivity was adjusted to appropriate levels with culture medium, and the cells were treated with these solutions immediately after the measurement of radioactivity.

2.3. Colony formation assay

To investigate the survival of cells following treatment, cells were harvested and suspended in medium, and diluted cells were inoculated into 6-well plates to examine the formation of colonies. Ten days later, colonies were fixed with ethanol and stained with 3% Giemsa solution. When cells were treated with PET drugs, each drug was administered for 6 h before the formation of colonies.

2.4. Micronucleus assay

To investigate the induction of micronuclei by irradiation with ^{18}F, exponentially growing cells in 6-well plates were treated with each PET drug. Samples were prepared as described previously [25]. After cells had been treated for 6 h, 2 μg/ml cytochalasin B was added for 24 h. They were then harvested and treated with 3 ml hypotonic (0.1 M) KCl for 20 min, and fixed with 3 ml methanol–acetic acid (5:1). The cell suspensions were centrifuged at 1200 rpm for 5 min, the supernatant was removed, and cells were then resuspended in 4 ml methanol–acetic acid solution and incubated on ice for 5 min. After further centrifugation, the supernatant was removed and 0.5–1 ml methanol–acetic acid solution was added. Cells were resuspended and a sample was placed onto slides and stained with 7.5% Giemsa for 20 min. The number of micronuclei per 1000 binucleated cells was counted.

2.5. Immunofluorescent staining of 53BP1

To estimate the induction of DNA DSB after the treatment with each PET drug, cells on 22 × 22 mm cover slips in 35-mm dishes were treated with 24 MBq/ml ^{18}F carried by each PET drug. At each time point, the cells were fixed with 4% formaldehyde in PBS, permeabilized for 10 min on ice in 0.5% Triton X-100 in PBS, and washed thoroughly with PBS. The cover slips were then incubated with an anti-53BP1 antibody (Bethyl Laboratories, TX, USA) in TBS-DT (20 mM Tris–HCl, 137 mM NaCl, pH 7.6, containing 50 mg/ml skim milk and 0.1% Tween-20) for 2 h at 37 °C. The primary antibodies were washed with PBS, and Alexa Fluor 594-labeled anti-rabbit IgG secondary antibodies (Invitrogen) were added. The cover slips were incubated for 1 h at 37 °C, washed with PBS, and sealed onto glass slides with 0.03 ml PBS containing 10% glycerol (Wako, Osaka, Japan) and 2 μg/ml DAPI (4′,6-diamidino-2-phenylindole; Invitrogen, CA, USA). The cells were examined using an Olympus fluorescence microscope (Olympus, Tokyo, Japan). The number of red foci for 53BP1 was counted on digitized images of Image J. The average number of foci in cells was determined in 600 cells from the three independent studies.

2.6. Statistical analysis

Statistical analysis was performed using the Student's *t* test.

3. Results

3.1. Analysis of the volume effects of ^{18}F in the medium

The biological effects of ^{18}F-FDG and ^{18}F-HF are caused not only by intracellular ^{18}F but also by irradiation from the outside of cells. The energy of γ-rays from ^{18}F is 511 keV; therefore, the existing radioactivity of ^{18}F in the medium is thought to contribute to cellular effects. In order to clarify the extent of the contribution of ^{18}F in the medium to cellular lethality, we used different volumes of media that contained the same concentrations (24 MBq/ml) of radioactivity originating from ^{18}F (Fig. 1A), and we compared the proportions of surviving cells among the different volumes. The number of radiation tracks may increase with the amount of medium. As shown in Fig. 1B, the proportion of surviving cells treated with 24 MBq/ml of ^{18}F-FDG was approximately 30% in every volume of medium, which was lower than for cells treated with ^{18}F-HF (approximately 50% survival) in all medium volumes. However, no significant differences in the proportions of surviving cells were observed among the different volumes of medium (Fig. 1B). This result suggested that the survival of ^{18}F-treated cells was influenced by ^{18}F that entered or adhered to, or was present in the vicinity of, the cells, but not by ^{18}F not in the vicinity of the cells.

3.2. Intracellular levels of ^{18}F-FDG and ^{18}F-HF

Intracellular levels of ^{18}F-FDG or ^{18}F-HF were examined by measuring the radioactivity of cells treated with each drug. The radioactivity of the medium in the cell culture dish was adjusted to 24 MBq/ml, and the intracellular incorporation of ^{18}F-drugs was examined at the time points indicated in Fig. 1C. The results obtained showed that ^{18}F-FDG was incorporated into cells in a time-dependent manner until 120 min after the start of treatment, and a decrease in radioactivity was observed after 120 min because of the decay of ^{18}F. When measured values in cells treated with ^{18}F-FDG were modified by decay compensation, the values showed a linear increase (Fig. 1C). This linearity indicated that ^{18}F-FDG accumulated in cells during the 6-h treatment period in our experimental conditions. However, in the case of ^{18}F-HF treatment, radioactivity was not detected in the cells at every time point. Therefore, we concluded that ^{18}F-HF did not accumulate in cells.

3.3. Different effects of lethality between ^{18}F-FDG and ^{18}F-HF

As shown in Fig. 1B, we demonstrated the different lethal effects between ^{18}F-FDG and ^{18}F-HF. To ensure that different biological effects were caused by different levels of ^{18}F accumulating in the cells, we performed a colony formation assay and micronucleus assay after treatment with ^{18}F-FDG or ^{18}F-HF for 6 h. As shown in Fig. 2A, the survival curve indicated that susceptibility

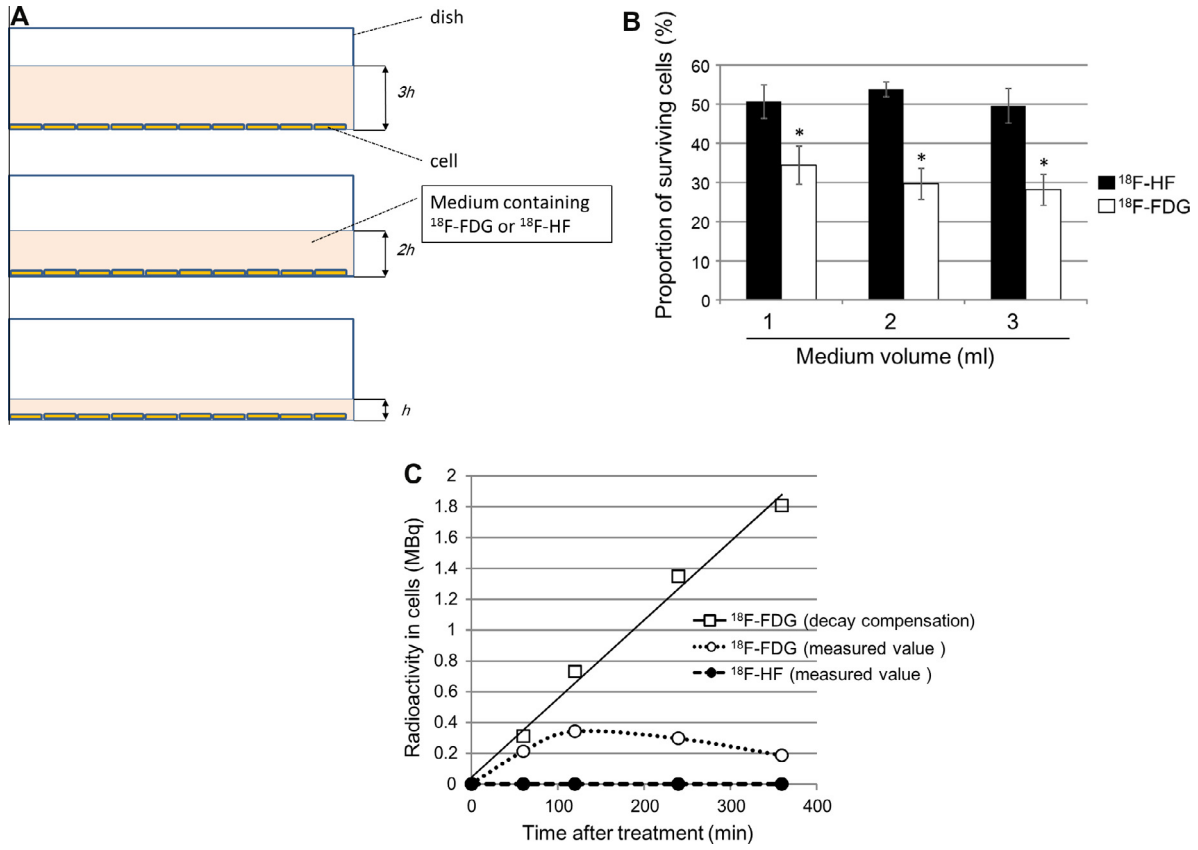

Fig. 1. (A) Illustration of treatment with ^{18}F-FDG or ^{18}F-HF in different volumes of medium. Cells were cultured at the bottom of each dish and were exposed to different volumes of ^{18}F in the medium, in addition to intracellular ^{18}F. The distance between the cells and medium surface increases two and three fold as the medium volume increased by 2 and 3 mL, resulting in two and three fold increased amounts of radiation tracks emitted from 18F in the medium around the cells adhered to the bottom of the dish. (B) Proportion of surviving cells after treatment with 24 MBq/ml of ^{18}F-FDG or ^{18}F-HF for 6 h. Average values (±SEM) were obtained from three independent studies. Significant differences were observed between ^{18}F-FDG and ^{18}F-HF-treatment for each medium volume (*$p < 0.05$ by the Student t test). (C) Intracellular ^{18}F radioactivity in cells treated with 1 ml of 24 MBq/ml ^{18}F-FDG or ^{18}F-HF at each time point after treatment (open and filled circles, respectively). The values after decay compensation of ^{18}F in ^{18}F-FDG-treated cells are indicated (the equation of the line is $y = 0.0051x + 0.0441$ ($R^2 = 0.9906$)).

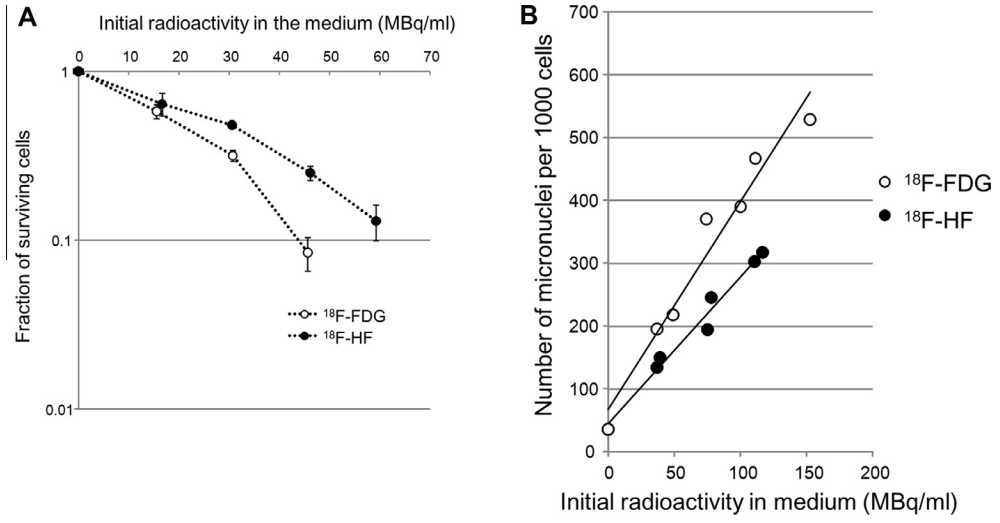

Fig. 2. (A) Fraction of cells surviving after treatment with ^{18}F-FDG or ^{18}F-HF for 6 h. Average values were obtained from three independent studies. (B) Micronucleus induction by treatment with ^{18}F-FDG or ^{18}F-HF for 6 h. Each plot presents data from three independent analyses. The equations for micronucleus induction after treatment with ^{18}F-FDG or ^{18}F-FDG are $y = 3.3023x + 67.329$ ($R^2 = 0.9591$) and $y = 2.336x + 44.518$ ($R^2 = 0.9782$), respectively.

to radiation was markedly higher in cells treated with ^{18}F-FDG than in cells treated with ^{18}F-HF (Fig. 2A). Because the lethal effects from ionizing radiation were caused by chromosome breakage, which results in micronucleus formation after cell division, we performed micronucleus assays after treatment with ^{18}F-FDG and ^{18}F-HF. As shown in Fig. 2B, micronucleus induction increased linearly

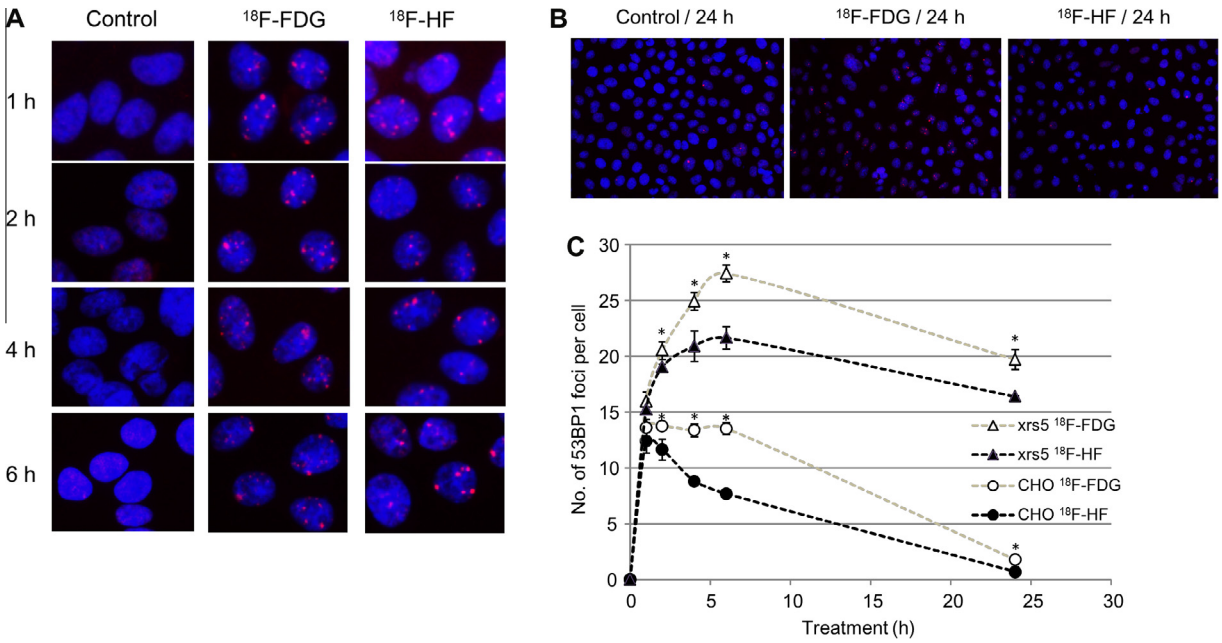

Fig. 3. (A) Fluorescence images of 53BP1 (red) on DAPI-stained nuclei (blue) in cells treated with 24 MBq/ml ^{18}F-FDG or ^{18}F-HF. In addition to non-treated (control) cells, cells 1, 2, 4 and 6 h after the treatment with ^{18}F-FDG or ^{18}F-HF are shown. (B) Cells 24 h after treatment with ^{18}F-FDG or ^{18}F-HF. (C) Average number of 53BP1 foci in cells treated with ^{18}F-FDG (open symbols) or ^{18}F-HF (closed symbols). The average number of 53BP1 foci induced by ^{18}F-FDG or ^{18}F-HF after the indicated times is shown in both CHO cells (circles) and repair-deficient xrs5 cells (triangles). Data obtained from three independent analyses. Significant differences were observed between ^{18}F-FDG and ^{18}F-HF treatment after 2, 4, 6, and 24 h in both cell lines ($^{*}p < 0.05$ by Student's t test). (For interpretation of the references to color in this figure legend, the reader is referred to the web version of this article.)

with the increase in radioactivity, and inductions by ^{18}F-FDG caused a greater level of micronucleus induction than ^{18}F-HF.

3.4. Estimation of DNA double-strand breaks after treatment with ^{18}F-FDG or ^{18}F-HF

Because DNA double-strand breaks (DSBs) are the main cause of the lethal effects of radiation, we next quantified the level of DNA DSBs using the formation of 53BP1 foci. As shown in Fig. 3A and B, clear 53BP1 foci were observed in the nuclei of cells treated with ^{18}F-FDG and ^{18}F-HF. The number of foci at each time point is summarized in Fig. 3C in Chinese hamster ovary (CHO) and Ku80-deficient xrs5 cells after treatment with ^{18}F-FDG or ^{18}F-HF. The number of foci in CHOs at 1, 2, 4, 6, and 24 h after treatment with ^{18}F-FDG was significantly larger than after treatment with ^{18}F-HF (Fig. 3C). In the case of xrs5 cells, the number of foci following treatment with both ^{18}F-FDG and ^{18}F-HF increased until 6 h after treatment, whereas no increases were observed after 2 h in CHO cells. Furthermore, the induction of foci after treatments with ^{18}F-FDG and ^{18}F-HF was significantly higher in xrs5 cells than in CHO cells because of repair deficits in DNA DSBs. Significantly larger numbers of foci were observed after treatment with ^{18}F-FDG for 4, 6, and 24 h than with ^{18}F-HF. These results suggested that the lethal effects observed in cells treated with ^{18}F-FDG or ^{18}F-HF could be attributed to the induction of DNA DSBs, and the induction of DSBs was greater with ^{18}F-FDG than with ^{18}F-HF.

4. Discussion

Estimating the levels of exposure using PET drugs labeled with ^{18}F has typically been conducted by following the Medical Internal Radiation Dose Committee (MIRD) method. In this model, the half-life time of ^{18}F (= 110 min) and the pharmaceutical compartment model for each characteristic of a PET drug in each organ were the main factors that are used to estimate exposure levels in organs [18]. This model is useful for the estimation of effective doses of ^{18}F-labeled drugs for patients [2,3]. On the other hand, each ^{18}F-labeled PET drug is fundamentally designed based on the "cellular accumulation theory" to expose specific areas such as the cytoplasm, membrane receptors, DNA and mitochondria; therefore, the distribution of ^{18}F, accumulation levels in cell populations, or effectiveness of uptake into cells should differ between carrier drugs when observed microscopically. In spite of the short half-life of ^{18}F, these differences in accumulation in cells lead to variations in dose exposure in a cell population. According to this view, the effective dose, which is the sum of the exposed dose in each cell, remains unclear until the accumulated level in individual cells is estimated. In the present study, we analyzed the induced levels of DNA DSBs, which are the main outcome of irradiation, in individual cells treated with two types of ^{18}F-labeled PET drugs, FDG and HF, with the same level of radioactivity. The results shown in Fig. 3C demonstrated that the induction of DNA DSBs by ^{18}F in cells treated with ^{18}F-FDG, which accumulated inside cells, was markedly higher than that by ^{18}F-HF, which can access but does not accumulate in cells because of the form of the fluorine ion. In addition, we showed that higher numbers of DNA DSBs induced by ^{18}F-FDG with higher radioactivity led to elevated levels of chromosomal damage and higher rates of cell death compared with ^{18}F-HF, as shown Fig. 2A and B. These results clearly showed that different accumulation levels at the microscopic cellular level led to differential biological effects.

With regard to ^{18}F, the atom firstly emits positrons, which then emit pair annihilation γ-rays; the positron is immediately converted to γ-rays during annihilation with an electron, releasing two γ-rays in opposite directions with an energy of 511 keV. Although it is clear that the energies of the positron from ^{18}F and secondary γ-rays are 0.64 MeV and 511 keV, respectively, the biological effect of these radiation types has not yet been reported. Therefore, our observation in the present study is useful for

understanding the contribution of the positron and secondary γ-rays from ^{18}F in cells. We demonstrated that cell survival was barely influenced by γ-rays emitted from different amounts of ^{18}F (^{18}F-FDG and -HF) in the medium (outside of the cell) (Fig. 1B). Because the concentrations (Bq/ml) of ^{18}F were the same even in different volumes (illustrated in Fig. 1A), the same amounts of ^{18}F could enter the cells and markedly contributed to cell survival rates of 50% and 30% for ^{18}F-HF and ^{18}F-FDG, respectively, as shown in Fig. 1B. ^{18}F that enters the cells can generate positron tracks that may affect DNA, markedly contributing to DNA DSBs and cell death commonly observed at these concentrations. These results clearly suggested that the intracellular levels of ^{18}F that accumulated in each cell may be indispensable factors for estimating the level of biological exposure.

The accumulation of these drugs was found to be affected by the type of cell and factors such as the functions and differentiation levels of cells. Although we showed data from CHO and xrs5 cell lines, the induced levels of DNA DSBs by ^{18}F-labeled PET drugs may differ between cell types. In order to determine the absorbed dose from each ^{18}F-labeled PET drug more accurately, it would be valuable to estimate the exposure levels by 53BP1 foci analysis, as shown in Fig. 3A and B, in other human cell lines and in 3D tissue models. In addition, we used only ^{18}F-FDG and ^{18}F-HF in the present study. It is important to estimate the relative exposure levels from ^{18}F-labeled PET drug that distribute to specific areas, such as DNA and mitochondria, in cells. These analyses are useful to not only understanding the safety of PET drugs but also the biological effect of positrons and secondary gamma rays from ^{18}F.

Disclosure

The authors declare that they have no conflict of interest.

Acknowledgments

This work was supported by grants for Scientific Research from the Ministry of Education, Culture, Sports, Science, and Technology, Japan (26461863, 24791317).

References

[1] H. Fukuda, T. Matsuzawa, Y. Abe, S. Endo, K. Yamada, K. Kubota, J. Hatazawa, T. Sato, M. Ito, T. Takahashi, R. Iwata, T. Ido, Experimental study for cancer diagnosis with positron-labeled fluorinated glucose analogs: [^{18}F]-2-fluoro-2-deoxy-D-mannose: a new tracer for cancer detection, Eur. J. Nucl. Med. 7 (1982) 294–297.
[2] A.A. Mejia, T. Nakamura, M. Itoh, J. Hatazawa, K. Ishiwata, T. Ido, M. Matsumoto, H. Watabe, S. Watanuki, S. Seo, Absorbed dose estimates in positron emission tomography studies based on the administration of ^{18}F-labeled radiopharmaceuticals, J. Radiat. Res. 32 (1991) 243–261.
[3] M. Michael, L.M. Peterson, M.L. Jeanne, M.L. Evans, J.S. Rasey, W.J. Koh, J.H. Caldwell, K.A. Krohn, M. Graham, Fluorine-18-fluoromisonidazole radiation dosimetry in imaging studies, J. Nucl. Med. 38 (1997) 1631–1636.
[4] P. Som, H.L. Atkins, D. Bandoypadhyay, J.S. Fowler, R.R. MacGregor, K. Matsui, Z.H. Oster, D.F. Sacker, C.Y. Shiue, H. Turner, C.N. Wan, A.P. Wolf, S.V. Zabinski, A fluorinated glucose analog, 2-fluoro-2-deoxy-D-glucose (F-18): nontoxic tracer for rapid tumor detection, J. Nucl. Med. 21 (1980) 670–675.
[5] D.S. Surasi, P. Bhambhvani, J.A. Baldwin, S.E. Almodovar, J.P. O'Malley, 18F-FDG PET and PET/CT patient preparation: a review of the literature, J. Nucl. Med. Technol. 42 (2014) 5–13.
[6] Y. Gulyas, C. Halldin, New PET radiopharmaceuticals beyond FDG for brain tumor imaging, Q. J. Nucl. Med. Mol. Imaging 56 (2012) 173–190.
[7] M. Nakajo, M. Nakajo, M. Jinguji, A. Tani, Y. Kajiya, H. Tanabe, Y. Fukukura, Y. Nakabeppu, C. Koriyama, Diagnosis of metastases from postoperative differentiated thyroid cancer: comparison between FDG and FLT PET/CT studies, Radiology 267 (2013) 891–901.
[8] G. Grunder, C. Fellows, H. Janouschek, T. Veselinovic, C. Boy, A. Brocheler, K.M. Kirschbaum, S. Hellmann, K.M. Spreckelmeyer, C. Hiemke, F. Rosch, W.M. Schaefer, I. Vernaleken, Brain and plasma pharmacokinetics of aripiprazole in patients with schizophrenia: an [18F]fallypride PET study, Am. J. Psychiatry 165 (2008) 988–995.
[9] L.S. Kegeles, M. Slifstein, W.G. Frankle, X. Xu, E. Hackett, S.A. Bae, R. Gonzales, J.H. Kim, B. Alvarez, R. Gil, M. Laruelle, A. Abi-Dargham, Dose-occupancy study of striatal and extrastriatal dopamine D2 receptors by aripiprazole in schizophrenia with PET and [18F]fallypride, Neuropsychopharmacology 33 (2008) 3111–3125.
[10] R.M. Kessler, M.S. Ansari, P. Riccardi, R. Li, K. Jayathilake, B. Dawant, H.Y. Meltzer, Occupancy of striatal and extrastriatal dopamine D2 receptors by clozapine and quetiapine, Neuropsychopharmacology 31 (2006) 1991–2001.
[11] P. Riccardi, R. Baldwin, R. Salomon, S. Anderson, M.S. Ansari, R. Li, B. Dawant, A. Bauernfeind, D. Schmidt, R. Kessler, Estimation of baseline dopamine D2 receptor occupancy in striatum and extrastriatal regions in humans with positron emission tomography with [18F] fallypride, Biol. Psychiatry 63 (2008) 241–244.
[12] E. Wallius, J. Tohka, J. Hirvonen, J. Hietala, U. Ruotsalainen, Evaluation of the automatic three-dimensional delineation of caudate and putamen for PET receptor occupancy studies, Nucl. Med. Commun. 29 (2008) 53–65.
[13] M. Baqir, V. Lowe, E.S. Yi, J.H. Ryu, ^{18}F-FDG PET scanning in pulmonary amyloidosis, J. Nucl. Med. (2014).
[14] A. Cortes-Blanco, C. Prieto-Yerro, R. Martinez-Lazaro, J. Zamora, A. Jimenez-Huete, M. Haberkamp, J. Pohly, H. Enzmann, J. Zinserling, V. Strassmann, K. Broich, Florbetapir (F) for brain amyloid positron emission tomography: highlights on the European marketing approval, Alzheimers Dement. (2014).
[15] S.M. Landau, B.A. Thomas, L. Thurfjell, M. Schmidt, R. Margolin, M. Mintun, M. Pontecorvo, S.L. Baker, W.J. Jagust, Amyloid PET imaging in Alzheimer's disease: a comparison of three radiotracers, Eur. J. Nucl. Med. Mol. Imaging (2014).
[16] F. Bretin, G. Warnock, M.A. Bahri, J. Aerts, N. Mestdagh, T. Buchanan, A. Valade, F. Mievis, F. Giacomelli, C. Lemaire, A. Luxen, E. Salmon, A. Seret, A. Plenevaux, Preclinical radiation dosimetry for the novel SV2A radiotracer [18F]UCB-H, EJNMMI Res. 3 (2013) 35.
[17] M. Shidahara, M. Tashiro, N. Okamura, S. Furumoto, K. Furukawa, S. Watanuki, K. Hiraoka, M. Miyake, R. Iwata, H. Tamura, H. Arai, Y. Kudo, K. Yanai, Evaluation of the biodistribution and radiation dosimetry of the 18F-labelled amyloid imaging probe [18F]FACT in humans, EJNMMI Res. 3 (2013) 32.
[18] W.W. Wooten, Radionuclide kinetics in MIRD dose calculations, J. Nucl. Med. 24 (1983) 621–624.
[19] T. Stiff, M. O'Driscoll, N. Rief, K. Iwabuchi, M. Lobrich, P.A. Jeggo, ATM and DNA-PK function redundantly to phosphorylate H2AX after exposure to ionizing radiation, Cancer Res. 64 (2004) 2390–2396.
[20] A.A. Goodarzi, A.T. Noon, D. Deckbar, Y. Ziv, Y. Shiloh, M. Lobrich, P.A. Jeggo, ATM signaling facilitates repair of DNA double-strand breaks associated with heterochromatin, Mol. Cell 31 (2008) 167–177.
[21] K. Suzuki, H. Okada, M. Yamauchi, Y. Oka, S. Kodama, M. Watanabe, Qualitative and quantitative analysis of phosphorylated ATM foci induced by low-dose ionizing radiation, Radiat. Res. 165 (2006) 499–504.
[22] S. Bekker-Jensen, N. Mailand, Assembly and function of DNA double-strand break repair foci in mammalian cells, DNA Repair (Amst.) 9 (2010) 1219–1228.
[23] M. Yamauchi, Y. Oka, M. Yamamoto, K. Niimura, M. Uchida, S. Kodama, M. Watanabe, I. Sekine, S. Yamashita, K. Suzuki, Growth of persistent foci of DNA damage checkpoint factors is essential for amplification of G1 checkpoint signaling, DNA Repair (Amst.) 7 (2008) 405–417.
[24] A.T. Noon, A. Shibata, N. Rief, M. Lobrich, G.S. Stewart, P.A. Jeggo, A.A. Goodarzi, 53BP1-dependent robust localized KAP-1 phosphorylation is essential for heterochromatic DNA double-strand break repair, Nat. Cell Biol. 12 (2010) 177–184.
[25] G. Kashino, K.M. Prise, G. Schettino, M. Folkard, B. Vojnovic, B.D. Michael, K. Suzuki, S. Kodama, M. Watanabe, Evidence for induction of DNA double strand breaks in the bystander response to targeted soft X-rays in CHO cells, Mutat. Res. 556 (2004) 209–215.